Bulletin of Earthquake Engineering
https://doi.org/10.1007/s10518-025-02301-y

ORIGINAL ARTICLE

A model for the simulated design of Turkish RC frame buildings in seismic vulnerability analysis

Serkan Hasanoğlu[1,2] · **Volkan Ozsarac**[1,2] · **Gerard J. O'Reilly**[1,2]

Received: 29 April 2025 / Accepted: 30 September 2025

Abstract
Seismic vulnerability modelling requires methodologies that account for changes in design practices over time and the inherent variability within building portfolios, including the differences in geometry, materials, and construction quality. Conventional models use different assessment approaches, classification systems, and representations of seismic loading and are often developed using a limited number of archetypal structural models to characterise an entire building class. As a result, these models tend to oversimplify individual building response, often fail to reflect building-to-building variability adequately, and do not account for multiple sources of uncertainty. To overcome these limitations, a collaborative and unified simulated design (SimDesign) framework for buildings has recently been introduced under the Built Environment Data (BED) initiative alongside an open-source Python implementation. Following the simulated design process, the framework generates numerical models in OpenSees for non-linear analyses, facilitating the development of vulnerability models for RC buildings. Leveraging its collaborative nature, this article presents the first country-specific extension of the framework for reinforced concrete (RC) frame buildings in Türkiye. More specifically, the historical and modern Turkish seismic design regulations are examined in detail, and specific design rules are integrated along with available statistical data on construction practices. Example applications were also conducted to assess the structural capacities associated with each implemented Turkish design class through non-linear pushover and dynamic analyses. The analysis outcomes revealed a consistent improvement in lateral force and ductility capacity over time, closely aligned with progressive enhancements in seismic code provisions and construction practices. Ultimately, this work has the potential to support more accurate seismic vulnerability modelling, which improves risk assessments and aids effective mitigation strategies for enhanced disaster resilience in the country.

Keywords Simulated design · Turkish seismic design codes · Reinforced concrete · Moment frames · Vulnerability modelling

Extended author information available on the last page of the article

Published online: 08 October 2025

1 Introduction

Understanding the seismic performance of RC frame buildings is a critical area of research in earthquake engineering, particularly in regions like Türkiye, which are prone to frequent and severe seismic activity. Damage observed in reinforced concrete (RC) frame structures after recent earthquakes (Yilmaz et al. 2024) have again underscored the importance of assessing the risks associated with existing buildings to predict and mitigate potential future damages and losses. By analysing factors such as structural design, construction materials, maintenance practices, and socio-economic conditions, vulnerability models provide critical insights into potential damage and inform effective disaster risk mitigation strategies (Martins and Silva 2021).

Fragility functions are central to physical vulnerability modelling, quantifying the probability of reaching or exceeding specific damage thresholds for different seismic intensity levels. These functions are developed using three main approaches: empirical, analytical, and hybrid methods. Empirical methods utilise structural damage data observed after earthquakes (Hancilar et al. 2013; Kircher et al. 1997; Rossetto and Elnashai 2003) but are often constrained by the availability of reliable post-earthquake damage data and accurate ground motion estimates. Analytical methods, on the other hand, utilise structural models and computational analyses to enable vulnerability assessments in regions with limited empirical data (Ayala et al., 2015; Erberik 2008; Nafeh & O'Reilly, 2023, 2024). Hybrid approaches combine the strengths of empirical and analytical methods (Kappos et al. 1998).

Among these, analytical methods have been widely adopted by researchers to study the vulnerability of RC frame structures in Türkiye. For example, Akkar et al. (2005) developed displacement-based fragility functions for low- and mid-rise RC frame buildings with infill walls using building data from the Düzce earthquake. Similarly, Kircil and Polat (2006) generated fragility curves for 12 mid-rise RC frame buildings in Istanbul, designed according to the Turkish Building Earthquake Code, published in 1975 (TBEC-1975). Erberik (2008) analysed 28 RC frame buildings constructed between 1970 and 1999 using the Düzce observed damage database (Ozcebe et al. 2003), defining building classes based on number of storeys and the presence of infill walls. Hancılar and Caktı (2015) examined mid- and high-rise RC frame buildings designed following TBEC-2007, employing multi-degree-of-freedom (MDOF) models to generate fragility curves for engineering demand parameters such as maximum peak storey drift and peak floor acceleration. Ucar et al. (2015) generated building capacity curves for 30 RC buildings, ranging from 3 to 8 storeys, based on data obtained through a walk-down survey in the city of Izmir.

While these studies provide valuable insights, they often rely on a limited number of representative structures. Moreover, traditional vulnerability models often depend on broad building class definitions and are developed using different numerical modelling and assessment approaches as discussed in Ruggieri et al. (2022). On the modelling side, various idealisations are employed, ranging from the simple equivalent single-degree-of-freedom (SDOF) systems, which are widely used in regional studies for their computational efficiency, to 2D-MDOF models, which strike a balance between realism and computational cost, and finally to detailed 3D-MDOF models, which provide the most comprehensive and realistic representation of structural behaviour, albeit at a higher computational demand. In terms of analysis approaches, methods generally include non-linear pushover and time history analyses, each with its own trade-offs between computational cost and ability to cap-

ture inelastic and dynamic response characteristics. All these factors lead to an inadequate representation of building-to-building variability and overlook critical sources of uncertainty. In addition, differences in adopted methodologies lead to a lack of harmonisation, hindering comparability and making the use of previously developed vulnerability models in risk assessments challenging, especially for large-scale applications. These limitations highlight the need for a systematic approach to vulnerability modelling, which accounts for the evolution of seismic design codes while comprehensively reflecting variability in building geometries and structural attributes, such as material properties.

To tackle some of these challenges, which are also relevant to other countries in Europe, the latest European exposure model (Crowley et al. 2020), developed under the Horizon 2020 SERA project (http://www.sera-eu.org/), introduced an enhanced taxonomy for RC frame buildings, incorporating seismic design code evolution and seismic demand zonation into building classifications as taxonomy attributes. Traditional exposure models primarily rely on morphological attributes (e.g., number of storeys, construction year, material, and structural system) derived from statistical data, surveys, image processing, or remote sensing. However, these attributes alone do not capture a building's expected lateral strength and ductility capacity. Previous approaches attempted to map ductility classes based on construction year and regional seismicity but lacked flexibility across time and geography. To address this, Crowley et al. (2021a, b) proposed a new mapping scheme that decouples seismic strength (lateral load coefficient, β) from seismic design principles (reflecting ductility-related aspects). In this classification, the latter is defined by the four design classes representing prevailing European seismic design practices over different periods. This harmonised framework accounts for seismic zonation changes, evolving design provisions, and construction practices over time. The approach introduced by Crowley et al. (2021a, b) improves the classification of RC buildings, but currently available exposure models still lack detailed information on the buildings, such as geometry and structural details. Simulated design procedures (Borzi et al. 2008; Del Gaudio et al. 2015; O'Reilly & Sullivan, 2018; Ruggieri et al. 2022; Verderame et al. 2010) can help overcome this limitation by reconstructing realistic structural configurations based on engineering practices of the time. To estimate the building design, this method requires only a few geometric variables and attributes, which can be randomly generated based on statistical data. Accordingly, this methodology was adopted during the development of vulnerability curves for low- to mid-rise RC frame buildings that are representative of general European construction practices and utilised in the 2020 European Seismic Risk Model (ESRM20) (Crowley, Dabbeek Crowley et al. 2021a, b). To capture the building-to-building variability within a building class, the geometric variables and attributes required for the design procedure were randomly generated based on existing statistical distributions.

However, it can be quickly recognised that statistical data on general building properties (e.g., span lengths, story heights, and material strengths) can vary significantly across countries and regions. Additionally, building codes and design practices differ globally, with seismic events often driving changes in national standards, revealing specific deviations from the generalised building class definitions. While existing simulated design procedures align with historical seismic design codes, they remain limited to country-specific applications and localised studies, lacking a generalised framework and supporting software tools for broader applicability. Another critical limitation is the mismatch between actual buildings and those generated strictly based on design rules. Factors such as material strengths,

stirrup spacing, and anchorage details, influenced by construction quality, significantly impact structural vulnerability yet remain underrepresented in many models. Additionally, numerical modelling choices influenced by construction quality are often absent from traditional vulnerability models, reducing their ability to produce realistic risk assessments. To overcome the limitations described above, building upon the developments of the SERA project, a collaborative and unified simulated design framework (SimDesign https://simdesign.builtenvdata.eu/) which offers extensibility to individual countries has been recently proposed along with the open-source Python implementation (Ozsarac et al. 2025).

Nevertheless, expanding the framework for individual countries requires a detailed understanding of the evolution of seismic design and construction practices. This knowledge is often only available through non-digitised texts written in the local language, or through well-known reference textbooks available at the time, or through acquired professional experience retrievable only through in-person interviewing and data collection. In this context, this study extends the SimDesign framework for RC frame buildings in Türkiye by integrating past and present Turkish seismic design regulations. Notably, this extension enables, for the first time, the simulated design of Turkish RC frame buildings while accounting for temporal and spatial variations in seismic design practices. Following the design process, the referred tools implementing the framework generate the OpenSees (McKenna et al. 2010; Zhu et al. 2018) numerical models that can then be used to perform non-linear analyses of the designed buildings and obtain probabilistic seismic demand models. These will ultimately support the development of fragility functions and vulnerability models for Türkiye.

The paper begins with an overview of past and present seismic design codes for RC frame buildings in Türkiye, followed by a short discussion of damage observations from some recent earthquakes. After that, specific information about the framework is explained in detail, with an emphasis on the data integrated for Turkish RC frame buildings. Finally, the framework's simulated design capabilities are showcased through two example applications that illustrate key differences among the examined design classes and underscore the significance of the attributes involved.

2 Evolution of seismic design codes and past damage observations in Türkiye

Türkiye is located in one of the most seismically active regions of the world, where tectonic activity is primarily governed by the interactions between Eurasian, Arabian, and African Plates, as illustrated in Fig. 1. The northward motion of the African and Arabian Plates generates compressional forces as they collide with the Eurasian Plate and leads to the westward motion of the Anatolian Plate along the North Anatolian Fault (NAF) and the East Anatolian Fault (EAF). Along its northern boundary, the Anatolian block moves westward relative to the Eurasian Plate at a rate of approximately 25 mm/yr, with most of this motion concentrated along the right-lateral strike-slip NAF. Similarly, along its southeastern boundary, the Anatolian block moves southwest relative to the Arabian Plate at a rate of about 10 mm/year along the left-lateral strike-slip EAF (Reilinger et al. 2006). The Aegean Graben System is another significant tectonic setting in the region, which is characterised by a normal faulting mechanism, further increases its high seismic activity.

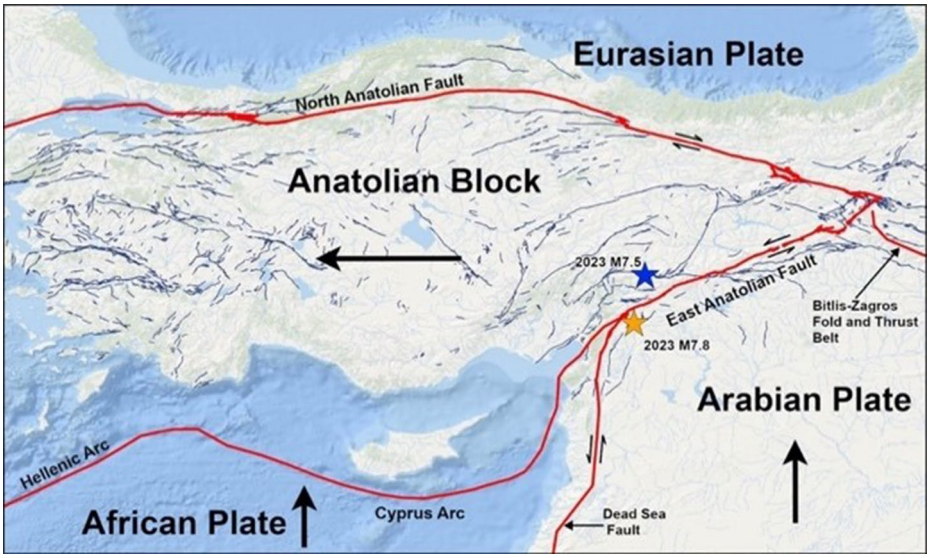

Fig. 1 Tectonic setting and major active fault systems in Türkiye (USGS, 2024)

As a consequence of its high seismic activity, Türkiye has experienced 21 earthquakes with magnitudes of 7.0 or greater since 1900. Among the most devastating were the 1939 M_w 7.8 Erzincan earthquake, the 1999 M_w 7.6 Izmit (Kocaeli) earthquake, and the recent 2023 M_w 7.8 and M_w 7.5 Kahramanmaraş earthquakes (depicted in Fig. 1), each resulting in a high level of damage and loss of life. For instance, the 1939 Erzincan earthquake caused over 32,000 fatalities and more than 100,000 injuries, while the 1999 Izmit earthquake resulted in 17,000 deaths and more than 50,000 injuries. Most recently, the 2023 Kahramanmaraş earthquakes led to catastrophic losses, with fatalities exceeding 50,000 and more than 100,000 injuries reported by United States Geological Survey (USGS, 2024).

2.1 Overview of design codes for RC frame buildings

Over the last decades, the building stock in Türkiye has undergone significant changes. Rapid urbanisation and population growth, particularly after the 1970s, have substantially increased RC construction. Eventually, as highlighted by recent studies (e.g., Bal et al. 2008; Yilmaz et al. 2024), RC frame buildings have become the most dominant building typology in the country, with the proportion of those constructed before the 1970s remaining negligible. However, this rapid urban expansion occurred with limited public awareness of seismic risks, resulting in the widespread construction of low-quality buildings in seismically active regions. This has been identified as one of the primary factors contributing to the devastating consequences of past earthquakes (Erdik 2001; Bayraktar et al. 2013; Yuzbasi 2024; Yilmaz et al. 2024). Accordingly, seismic design codes have undergone serious revisions over time alongside global advancements in earthquake engineering, integrating the key design concepts with each revision, as summarised in Table 1. Although each code was published as a standalone regulation rather than as a formal revision of the preceding one, some versions shared notable similarities. For example, the pre-1968 codes had closely

Table 1 Evolution of Turkish seismic design codes

Code	General Information	RC Frame Buildings
1940	• Introduced earthquake load calculation procedure via lateral load coefficients	• No specific limitations
1944	• Introduced building height limits based on structural system	• No specific limitations
1949	• Introduced a seismic zonation map with three zones for which different ranges of lateral load coefficients are provided • Introduced a limitation on the number of storeys based on the seismic zone	• No specific limitations
1953	• Specified the live load reduction factors based on building typology • Specified the lateral load coefficient values as a function of soil class, structural characteristics, and earthquake zone	• No specific limitations
1961	• Revised the live load reduction factors • Revised the procedure for determining lateral load coefficient	• No specific limitations
1968	• Introduced a dedicated section for RC buildings, although not detailed • Updated the seismic zonation map with four zones • Revised the procedure for calculating lateral load coefficient to account for spectral shape and building importance for the first time • Introduced an expression for distributing lateral loads at floor levels based on floor weights and levels	• Specified minimum dimensions for beams and columns • Specified minimum longitudinal reinforcement for beams • Enforced use of transverse reinforcement in columns, beams and joints without specifying limits • Prevented use of hollow block slabs for buildings at the first- and second-degree seismic zones
1975	• First modern earthquake code • Updated the seismic zonation map with five zones • Explicitly mentioned the ductility at both structural and component levels • Revised procedure for calculating the seismic loads with more detailed consideration of soil conditions and dynamic properties of structure	• Specified minimum dimensions and reinforcement ratios for all types of structural members • Introduced detailed design principles for seismic-resistant detailing with emphasis on the importance of confinement • Introduced quantitative expressions for ductile design
1998	• Explicitly defined design earthquake • Introduced elastic design spectrum • Defined structural-system-specific behaviour factors • Introduced seismic load reduction factor • Introduced capacity design concept • Quantitatively defined structural irregularities • Revised the seismic zonation map • Introduced mode superposition and time history analysis methods	• Defined minimum concrete strength as C20 for buildings at first- and second-degree seismic zones • Defined stricter rules for shear design • Defined more detailed rules for reinforcement detailing • Reduced the maximum axial load ratio limit for columns • Provided design expressions for the “strong column-weak beam” principle
2007	• Added chapters on structural assessment and retrofitting	• Introduced minor updates to the design expressions • Defined minimum concrete strength as C20 for all buildings

Table 1 (continued)

Code	General Information	RC Frame Buildings
2018	• Introduced modern seismic hazard map with spectral acceleration coefficients • Introduced site-specific design spectra • Introduced vertical design spectrum • Introduced performance-based design • Defined structural-system-specific overstrength and behaviour factors	• Defined stiffness modifiers to account for concrete cracking • Reduced the maximum axial load ratio limit for columns • Defined stricter rules for shear design • Defined minimum concrete strength as C25 for all buildings

aligned provisions, and the 1998 and 2007 codes were largely similar, particularly in their RC design requirements.

The country's first building code was introduced in 1940 following the destructive 1939 Erzincan earthquake. This was based on the Italian building code of that time (Cansiz 2022; Yilmaz et al. 2024). After this code, subsequent revisions (1944, 1949, 1953, 1961), driven mainly by significant earthquakes such as Tokat-Erbaa (1942), Bolu-Gerede (1944), Muş-Varto (1946), Karlıova-Bingöl (1949), introduced some level of changes in building design and construction regulations. However, all the codes before 1968 lacked explicit design provisions for RC buildings, aside from a few minor constraints. The 1968 seismic code marked a significant milestone by introducing a dedicated chapter for RC structures, although it remained limited in detail.

After several early seismic design regulations, Türkiye's first modern and comprehensive seismic design code was published in 1975 (TBEC-1975). This code was the first to explicitly mention of ductility at the structural and member levels. Moreover, between 1975 and 2000, two RC design and construction codes, TS500-1975 and TS500-1984, were also in effect. Prior to 1975, RC elements were designed solely based on the allowable stress method, which was also adopted in TS500-1975. Notably, TS500-1984 introduced new improvements, particularly refining RC design practices with the introduction of the ultimate strength design method. While the allowable stress method was still permitted, the code explicitly encouraged the adoption of the ultimate strength method. As a result, after the mid-1980s, design engineers began to use the ultimate strength design instead of the allowable stress approach (Ilki and Celep 2012).

As seismic design practices continued to evolve, TBEC-1998 was released, incorporating modern design concepts such as capacity design principles, seismic load reduction factor and advanced analysis methods such as mode superposition and non-linear time history analysis. This code also enhanced the shear design provisions for RC elements. Furthermore, TBEC-1998 introduced two ductility levels to be followed in building design: high (DCH) and moderate (DCM) ductility. The choice of ductility level in design was determined based on the seismic zone in which the building was located. High ductility was mandatory for RC frame buildings in first- and second-degree seismic zones, whereas moderate ductility was permitted in third- and fourth-degree seismic zones, though high ductility remained an option. The main difference between the two was the consideration of capacity design rules, particularly the strong column-weak beam principle and capacity-based shear force design of beams and columns.

Subsequently, the latest version of the TS500 series, TS500-2000, was released with new provisions on RC design and construction rules. Most notably, it eliminated the use of the allowable stress design approach by making the ultimate strength design method mandatory

for RC structures. Later, TBEC-2007 was released, introducing new chapters by addressing the seismic assessment and retrofitting of existing structures. However, it included only minor updates to the design rules for RC frame buildings.

Finally, TBEC-2018 brought significant advancements by incorporating a modern spectrum-based seismic hazard map and adapting a performance-based design approach. It provided stricter ductility requirements and, for the first time, accounted for cracked stiffness modifiers in design calculations. In this code, RC frame buildings in Earthquake Design Class 1 and Earthquake Design Class 2 (this classification of design classes is similar to the seismic zonation in previous codes) have been enforced to be designed with high ductility level while design with moderate ductility was permissible for Earthquake Design Class 3 and Earthquake Design Class 4, though high ductility remained an alternative again. Besides, the code required the consideration of the overstrength factor in the calculation of seismic load reduction factor and shear design for beams and columns.

In addition, it is also important to note that β values, or lateral load coefficients, defined as the ratio of lateral earthquake load to total weight of the structure, have significantly changed with each code revision. In particular, Fig. 2 illustrates the variation of β values across the design codes released between 1949 and 2018, considering a hypothetical four-story RC frame building located on stiff sandy soil in the Zeytinburnu district of Istanbul. It should be noted that slight variations of the given values may occur due to assumptions regarding the dynamic characteristics of the building and the soil type. Furthermore, it should also be considered that the region was designated as a second-degree seismic zone until 1996. After 1996, it has been designated as a first-degree seismic zone. The increasing trend in lateral load coefficient indicates the continuous improvement of considered earthquake loads in RC building design with time.

2.2 Damage observations from past earthquakes

Although seismic design codes have incorporated the best design provisions of their era, particularly for the buildings built after 1975, the RC building stock has experienced catastrophic losses in past earthquakes (e.g., the 1999 Kocaeli, 2023 Kahramanmaraş earthquakes), particularly due to poor construction quality. Based on the damage observations in post-earthquake reconnaissance studies, critical deficiencies can be revealed, which are important to capture when performing simulated design of existing building portfolios.

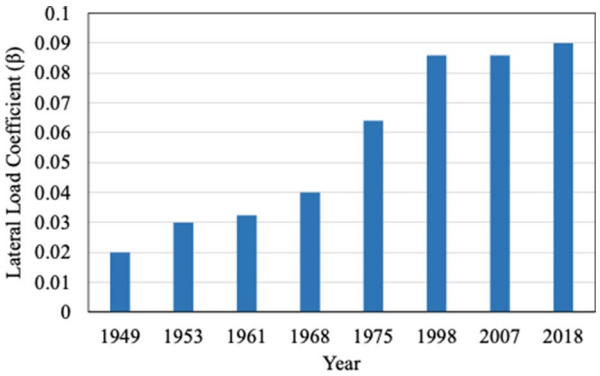

Fig. 2 Variation of the lateral load coefficient based on different Turkish design codes

Among these studies, Ilki and Celep (2012) identified issues such as inadequate lateral load capacity due to poor concrete strength and insufficient reinforcement, limited lateral stiffness from weak frame formations, lack of ductility, and the presence of soft and weak storeys, particularly on ground floors, based on damage assessments conducted after several earthquakes, including the 1999 Kocaeli earthquake. Similarly, Bayraktar et al. (2013) reported some deficiencies following the 2011 Van earthquake, where damage was concentrated in areas with ground failures, soil liquefaction, poor concrete strength, unribbed reinforcement, inadequate beam-column joint detailing, and strong beam–weak column configurations. Other contributing factors included short columns, weak walls, improper lap splices, and insufficient separation distances between adjacent buildings, which lead to pounding damage. Yakut et al. (2022) highlighted soft and weak ground floors and excessive column corrosion as primary causes of damage following the 2020 Samos earthquake in Izmir. Likewise, Binici et al. (2023) analysed the damage caused by the 2023 Kahramanmaraş earthquakes and attributed collapses in pre-2000 buildings to insufficient lateral rigidity and poor beam-column joint detailing. For post-2000 buildings, they identified issues such as using hollow block slabs, poor lateral force distribution, underestimation of seismic demands, and inadequate local soil investigations.

Based on these past damage observations, the most critical structural issues can be shown as low concrete strength, inadequate reinforcement detailing, weak beam-column connections, improper lap splices in critical regions, and the presence of soft and weak storeys, particularly on ground floors. These deficiencies were primarily found in the buildings constructed before 2000, as the 1999 Kocaeli and Düzce earthquakes affected the general public by highlighting the critical importance of compliance with seismic design codes. Following the 1999 earthquakes, several regulatory improvements were introduced to enhance construction quality, including the mandatory use of ready-mix concrete and ribbed steel reinforcement bars, as well as the implementation of mandatory construction inspections. The effectiveness of these regulatory measures was evident during the 2023 Kahramanmaraş earthquakes (Yilmaz et al. 2024), where buildings designed under new regulations exhibited improved seismic performance compared to older ones.

3 Integration of Turkish RC frame data into SimDesign framework

The SimDesign framework follows a structured four-step process (see Fig. 3) to integrate seismic design practices into a computational modelling environment. In the first step, a dataset that defines the general characteristics of buildings in a specific region is generated to guide the simulated design. More specifically, this includes three primary attributes,

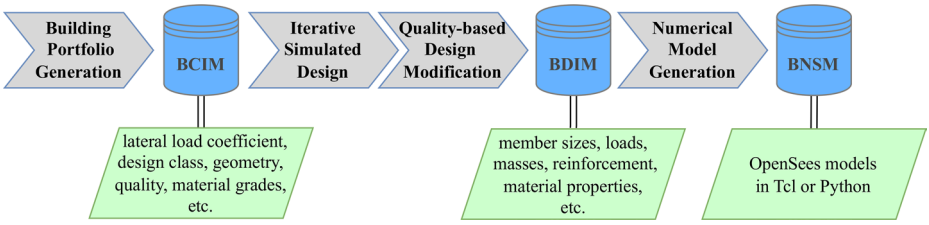

Fig. 3 General overview of the workflow defined in the SimDesign framework

which are number of storeys, β, and design class, representing seismic design practices and rules to be considered. Additionally, it includes secondary attributes, such as material grades and construction quality, along with geometric variables (e.g., in-plan configurations and storey heights). Together, the secondary attributes and geometry variables reflect the building-to-building variability and are established through random sampling from probability distributions specific to a given design class. At the end of this step, the generated dataset for the building portfolio, or the building realisations, is stored in the *Building Class Information Model (BCIM)* database.

Following dataset generation, each building realisation undergoes a simulated design process that replicates an engineer's supposed decision-making approach. Structural member dimensions and reinforcement details are iteratively determined to ensure compliance with national code provisions and design practices. After completing the design process, quality-based modifications are applied to account for variations in material properties and reinforcement detailing based on the construction quality level, which can be classified as Low, Moderate, or High. The finalised design details, including material properties, reinforcement configurations, and section dimensions, are stored in the *Building Design Information Model (BDIM*) database.

In the final step, the building design data are utilised to generate 3D non-linear numerical models in OpenSees (McKenna et al. 2010; Zhu et al. 2018), incorporating state-of-the-art modelling approaches. For each building, modal and non-linear static pushover analysis routines are developed alongside the numerical models and collectively stored in the *Building Non-linear Structural Model (BNSM)* database.

The following subsections detail this workflow with a particular focus on the Turkish RC frame design classes integrated into the framework. First, the general criteria for defining specific design classes will be discussed. This will be followed by a summary of the building portfolio generation process. Next, the iterative design process will be detailed. For more detailed information about the SimDesign framework and its Python implementation (available at https://github.com/builtenvdata/simulated-design), readers are encouraged to refer to the reference publication (Ozsarac et al. 2025) that describes the overall initiative in a broader context.

3.1 Determination of the Turkish RC frame design classes

Modern seismic design codes generally provide distinct design provisions for different target ductility levels, which are categorised under ductility classes such as medium (DCM) and high (DCH). Even when the same target ductility levels are retained across consecutive codes, as in TBEC-2007 and TBEC-2018, the corresponding design provisions to achieve these may vary significantly. As a result, designs based on different code versions may exhibit notable differences, even when targeting the same ductility level. Therefore, incorporating the construction period along with the ductility level is a better strategy for determining country-based design classes. Based on this, the Turkish RC frame design classes are proposed, as shown in Table 2, by considering both the construction period, which is considered by utilising design code and practices in effect, and ductility level, whenever the latter is explicitly specified in the seismic code.

It is important to note that the number of buildings constructed before 1970s is negligible compared to Türkiye's total RC frame building stock (e.g., Bal et al. 2008 and Yilmaz

Table 2 Considered Turkish design classes of RC frame buildings in the framework

Design Class	Construction Period	Ductility Level	Reference Codes
tr_7599	1975–1999	Low	TBEC-1975 TS500-1984
tr_0018_dch	2000–2018	High	TBEC-1998 TS500-2000
tr_0018_dcm	2000–2018	Moderate	TBEC-1998 TS500-2000
tr_post18_dch	After 2018	High	TBEC-2018 TS500-2000
tr_post18_dcm	After 2018	Moderate	TBEC-2018 TS500-2000

et al. 2024). Therefore, the design classes proposed herein encompass constructions built after 1975. The "tr_7599" design class represents RC frame buildings constructed between 1975 and 1999, incorporating the design rules and procedures outlined in TBEC-1975 and TS500-1984. Due to the widespread presence of poor-quality constructions in this period, the design outcomes attained in the simulations of this class are adjusted by calibrating the quality-based design modification process, the details of which will be given in following sections. Later on, although TBEC-1998 was the following published seismic code after TBEC-1975, the upper limit of the construction period was set to 2000 for two reasons: (i) widespread non-compliance with seismic design codes before 2000 and (ii) the introduction of TS500-2000, which brought significant updates to RC design and general RC construction practice. Additionally, while both the allowable stress and ultimate strength methods were used during this period, the latter was implemented in this design class, assuming that the buildings constructed after the mid-1980s constitute a larger portion of the current RC building stock (Bal et al. 2008).

For buildings constructed after 2000, the Turkish design classes integrated into the framework incorporate both ductility level and construction period, as seismic codes began explicitly defining ductility classifications starting with TBEC-1998 and continued through TBEC-2007 and TBEC-2018. For the "tr_0018_dch" and "tr_0018_dcm", representing buildings constructed between 2000 and 2018, the design rules from TBEC-1998 (which remained almost identical in TBEC-2007 for RC frame design) were applied, along with some provisions from TS500-2000. The main distinction between these two classes was the implementation of capacity design rules. Similarly, for the "tr_post18_dch" and "tr_post18_dcm", the rules from TBEC-2018 and TS500-2000 were implemented, with the main difference again being the use of capacity design principles. It is important to note that in all design classes discussed above, seismic design codes were prioritised over TS500 provisions when determining design parameters.

3.2 Building portfolio generation process

The building portfolio generation process begins by defining the portfolio size and the primary attributes that characterise the building class. Next, the framework generates samples of the secondary attributes (i.e., beam, column, and slab types, material grades and construction quality level) and the variables describing the building geometry (i.e., bay widths, story heights, and layout ID, representing the in-plan configuration). As illustrated in Fig. 4, this sampling process relies on random generators and decision trees developed based on experi-

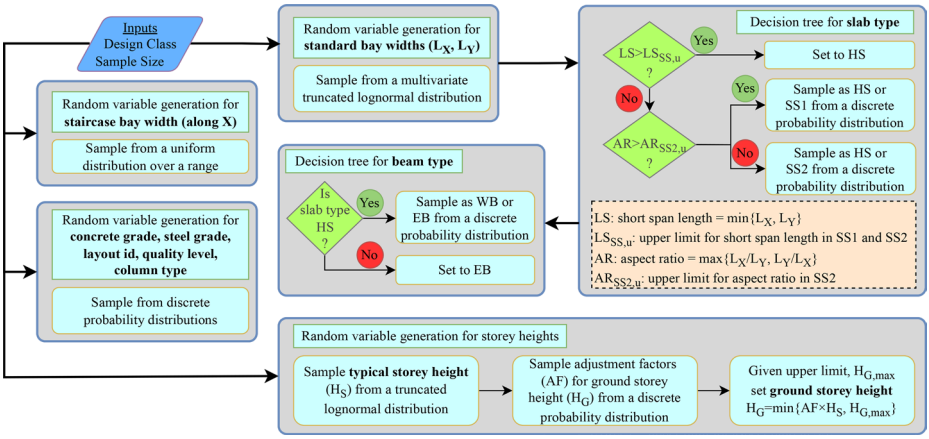

Fig. 4 Illustration of sampling processes for generating the BCIM data, with sampled data highlighted in bold

ence and engineering judgement. The random generators employ probability distributions to model the overall characteristics of the building stock, while decision trees reflect typical design-related assumptions.

Consequently, for each proposed design class, the probabilistic model parameters have been defined and integrated into the SimDesign framework. A complete list of input parameters is provided in Table A-1 of the Appendix. For example, the default values for each parameter in the "tr_post18_dch" class are given in Tables A-2 to A-9. However, the values for other design classes can be accessed on the GitHub repository[1]. To achieve this, statistical data on various structural attributes of Turkish RC frame buildings were primarily gathered from existing literature (Azak et al. 2014; Bal et al. 2008; Meral 2019; Ozmen et al. 2015). Among these, Bal et al. (2008) investigated the data collected from more than 1400 RC buildings from the Marmara Region to characterise the key attributes of this construction typology. The study provided detailed statistical data on a range of structural parameters including material properties, beam depth, storey height, etc., that are essential for developing representative building models. Given the thorough evaluation of the statistical parameters and the extensive scope of the work, it was selected as the primary reference in the present study for defining probabilistic input parameters. In cases where sufficient information was not available or for validation purposes, additional referenced studies were also consulted to supplement the data. Furthermore, relevant design codes and engineering judgment were incorporated when necessary. The following text details the underlying assumptions and methodologies used to define these inputs.

In terms of spatial configuration, bay widths in the framework were classified into two types: staircase bay width and standard bay width. Based on engineering judgment, a uniform probability distribution was assigned for staircase bay width, with lower and upper bounds of 2.8 and 3.2 m. For standard bay width, statistical data exist in the literature were analysed, and it was observed that the available data does not precisely represent standard

[1] Available on the following GitHub repository:
https://github.com/builtenvdata/simulated-design/blob/main/simdesign/rcmrf/bcim/data.

beam lengths. Instead, they also include other beam types, such as staircase span beams and tie beams, which are generally shorter. As a result, the mean values and the distribution types of beam length in these studies do not accurately reflect the specific case here. To address this, the statistical data given by Bal et al. (2008) were adjusted, and the modified parameters were used as default values in a multi-variate truncated lognormal distribution, which accounts for the correlation between the two perpendicular beam lengths and applies truncation at specified bounds to ensure realistic geometrical configurations.

Regarding slab classification, the framework considers three slab types by default: one-way cast-in-situ slabs (SS1), two-way cast-in-situ slabs (SS2), and precast joist slabs with ceramic blocks (HS). While precast joist slabs with ceramic blocks are uncommon in Turkish construction practice, they have similar structural characteristics to hollow block slabs (asmolen slab), which is a common type in Türkiye. These slabs are primarily used for economic and architectural reasons; however, their use has been restricted to specific conditions in recent seismic codes due to their poor earthquake performance, particularly due to their inability to sustain rigid diaphragm behaviour. To comply with seismic code restrictions, hollow block slabs are excluded from the sampling process for "tr_0018_dch" and "tr_post18_dch" design classes with the default values (see Table A-9) assigned in slab typologies while they are permitted in other design classes. The selection of slab types, including HS slab, is determined based on the following criteria:

- If the short span length of a slab exceeds a predefined short span length (e.g., 6 m), the HS slab is automatically assigned.
- Otherwise, the slab type is determined based on predefined discrete probability distributions. Specifically, if the aspect ratio of the slab is greater than a limit value (e.g., 2), the slab type is assigned as either SS1 or HS according to the predefined probability ratio. Similarly, if the aspect ratio is less than the limit value, the slab type is determined as either SS2 or HS based on the predefined ratio. These ratios are assumed by engineering judgment.

Beam types are determined based on the slab type. For SS1 and SS2 slabs, only emergent beams are assigned. In the case of HS slab type, wide beams (WB) are automatically assigned, as they are predominantly used with asmolen slabs in Turkish construction practice (see "wb_prob_given_hs" in Table A-1). It is important to note that external and staircase beams are always determined as emergent beam (EB), even when asmolen slabs are used in the structure. Additionally, the framework supports two RC column types: square and rectangular columns. Since square columns are rarely used in Turkish RC construction, comprising approximately 5% of the building stock (Azak et al. 2014), a default discrete probability value of 0.05 is given for square column selection across all Turkish RC frame design classes.

Additionally, material grades (i.e., reinforcing steel or concrete) used in each design class were determined based on the material types specified in TS500 while also considering the material grade restrictions imposed by seismic design codes. The discrete probability distribution values for each material grade were assumed based on engineering judgment and existing material strength distribution data from the literature (Bal et al. 2008; Meral 2019; Ozmen et al. 2015). Beyond material grades, construction quality level (high, moderate, low) is another attribute in the framework that directly affects the finalised structural mod-

els. More specifically, parameters such as stirrup spacing, concrete cover, mean compressive concrete strength and mean reinforcing steel yielding strength (for both the longitudinal and the transverse reinforcements) are adjusted using the quality factors (based on quality level) to establish expected in-situ values, which are then incorporated into numerical modelling. For this purpose, discrete probability values for quality levels were assumed by engineering judgment.

Regarding variations in storey height, Bal et al. (2008) investigated a dataset of 938 sample buildings by grouping them as compliant and non-compliant based on whether their construction period was before or after 2000. For typical storey height (upper floors), they found that both building groups had the same mean value, and eventually, they proposed a lognormal distribution with a mean and coefficient of variation value of 2.84 m and 8%. Additionally, they examined the ground storey height to typical storey height ratio for both emergent and wide beam cases across the two building groups. Their findings indicated that this ratio was significantly lower in the buildings constructed after 2000 due to the new constraints introduced in TBEC-1998, which aimed to mitigate soft storey behaviour by imposing stricter design limitations. To incorporate these variations within the framework, discrete probability distributions were employed for the ground storey height to typical storey height ratio, which is used to determine ground storey height by multiplying it with typical storey height. The default values were defined by using the data provided by Bal et al. (2008) for each Turkish RC frame design class as follows:

- For the "tr_7599" design class, the mean values of the ratios belonging to non-compliant buildings with emergent beams and non-compliant buildings with wide beams were adopted.
- For the "tr_0018_dch" and the "tr_post18_dch" design classes, the ratios corresponding to compliant buildings with emergent beams were used.
- For the "tr_0018_dcm" and the "tr_post18_dcm" design classes, the mean values of the ratios from compliant buildings with emergent beams and compliant buildings with wide beams were utilised.

After completing all sampling procedures, the BCIM dataset is generated with the specified sample or portfolio size. This dataset includes detailed information on all attributes and geometry variables for each building to guide the design process. However, users have the flexibility to modify all these default values, which is particularly useful when more accurate or region-specific data is available.

3.3 Iterative simulated design process with quality modifications

Following the sampling procedures, the spatial configurations of structural members (e.g., beams, columns, and slabs) were defined based on the assigned geometric variables, such as plan layout and storey heights. The structural design process is then carried out through an iterative procedure as detailed in (Ozsarac et al. 2025). It begins by assigning preliminary member dimensions based on seismic code requirements (see Tables 3 and 4), engineering practice rules in structural design, and anticipated gravity loads, including permanent and live loads. At this stage, section uniformisation, a common practice in structural engineering, is also applied to ensure consistent column dimensions throughout the building height

Table 3 Column design parameters in seismic and RC design codes in Türkiye

Parameter	TBEC-1975	TBEC-1998	TBEC-2018	TS500-1975	TS500-1984	TS500-2000
ρ_{min}	0.01	0.01	0.01	0.005	0.008	0.01
ρ_{max}	0.04	0.04	0.04	0.03	0.04	0.04
c_{min}	25 cm	25 cm	30 cm	20 cm	25 cm	25 cm
$A_{c,\,min}$		max(75000 mm², $N_{dm}/(0.5f_{ck})$)	$N_{dm}/(0.4f_{ck})$		$N_{dm}/(0.6f_{ck})$	$N_{dm}/(0.9f_{cd})$
$\Phi_{l,\,min}$			14 mm	14 mm		14 mm
$l_{c,\,min}$	max (c_{max}, $l_n/6$, 45 cm)	max(c_{max}, $l_n/6$, 50 cm)	max($1.5c_{max}$, $l_n/6$, 50 cm)			
$s_{c,\,min}$	5 cm	5 cm	5 cm			
$s_{c,\,max}$	10 cm	min(10 cm, $c_{min}/3$)	min(15 cm, $c_{min}/3$, $6\Phi_{l,\,min}$)			
$s_{m,\,max}$	min(20 cm, $c_{max}/2$, $12\Phi_{l,\,min}$)	min(20 cm, $c_{min}/2$)	min(20 cm, $c_{min}/2$)	min(25 cm, c_{min}, $12\Phi_{l,\,min}$)	min(20 cm, $12\Phi_{l,\,min}$)	min(20 cm, $12\Phi_{l,\,min}$)
$\Phi_{t,\,min}$	8	8	8	$\Phi_{l,\,max}/3$	$\Phi_{l,\,max}/3$	$\Phi_{l,\,max}/3$
$V_{d,\,max}$		$0.22A_{c,\,eff}\times f_{cd}$	$0.85A_{c,\,eff}\times f_{ck}^{0.5}$		$0.22A_{c,\,eff}\times f_{cd}$	$0.22A_{c,\,eff}\times f_{cd}$
$c_{c,\,min}$				20 mm	25 mm	25 mm
e_{min}					$0.1c_{max}$	$15+0.03c_{max}$
χ			0.7			

$A_{c,\,min}$: minimum column section area, $A_{c,\,eff}$: effective column section area, $c_{c,\,min}$: minimum concrete cover, c_{min}: minimum section dimension, c_{max}: maximum section dimension, e_{min}: eccentricity, f_{ck}: characteristic concrete strength, f_{cd}: design value of concrete strength, l_n: net column length, $l_{c,\,min}$: minimum confinement zone length, N_{dm}: maximum axial design load, $s_{c,\,min}$: minimum transverse bar spacing at confinement zone, $s_{c,\,max}$: maximum transverse bar spacing at confinement zone, $s_{m,\,max}$: maximum transverse bar spacing at midspan, $V_{d,\,max}$: maximum design shear force, ρ_{min}: minimum longitudinal reinforcement ratio, ρ_{max}: maximum longitudinal reinforcement ratio, $\Phi_{l,\,min}$: minimum longitudinal bar diameter, $\Phi_{l,\,max}$: maximum longitudinal bar diameter, $\Phi_{t,\,min}$: minimum transverse bar diameter, χ: cracked section rigidity coefficient

and uniform beam sections across continuous spans. These initial dimensions serve as the baseline for further design iterations.

After completing the preliminary design, an elastic numerical model of the building is established. To better approximate the actual structural behaviour, section stiffness values are adjusted using cracked section coefficients when required by seismic design codes (e.g., Table 4.2 in TBEC-2018). Subsequently, linear elastic analyses are performed for each load case, in which seismic loads are applied using the equivalent lateral force method (implemented through the previously described β coefficient). The resulting internal member forces are then combined by superposition in accordance with the load combinations specified in seismic codes (see Table B-2 and Table B-3 in the Appendix) to obtain the design forces. Finally, the envelope of these forces is also determined for use in subsequent design calculations and verifications.

Once the design forces are established, the next step involves verifying whether the selected section dimensions are adequate under the applied design loads. This verification assesses economic feasibility based on engineering rules of thumb and ensures compliance with allowable design shear force limits (see $V_{d,\,max}$ in Tables 3 and 4) specified by seismic code provisions. Upon section verification, the required longitudinal and transverse reinforcements for beam and column sections are determined. In design classes incorporat-

Table 4 Beam design parameters in seismic and RC design codes in Türkiye

Parameter	TBEC-1975	TBEC-1998	TBEC-2018	TS500-1975	TS500-1984	TS500-2000
$b_{h,\,min}$	30 cm	max(30 cm, $3t_{slab}$)	max(30 cm, $3t_{slab}$)			max(30 cm, $3t_{slab}$)
$b_{h,\,max}$		min($3.5b_w$, $l_n/4$)	min(3.5bw, $l_n/4$)			
$b_{w,\,min}$	20 cm	25 cm	25 cm			20 cm
$b_{w,\,max}$		$c_{wp} + b_h$	$c_{wp} + b_h$			$c_{wp} + b_h$
ρ_{min}	S220:0.005 S420:0.003	f_{ctd}/f_{yd}	$0.8f_{ctd} / f_{yd}$		$1.2/f_{yd}$	$0.8f_{ctd}/f_{yd}$
ρ_{max}		0.02	0.02			0.02
Θ_{max}	3	2	2			
$\Phi_{l,\,min}$	12	12	12		10	12
$\Phi_{t,\,min}$	8	8	8			
$l_{c,\,min}$		$2b_h$	$2b_h$			$2b_h$
s_{max}	min(b_w, $b_h/2$)	min($8\Phi_l$, $b_h/4$, 15 cm)	min($8\Phi_l$, $b_h/4$, 15 cm)			min($8\Phi_l$, $b_h/4$, 15 cm)
$\rho_{t,\,min}$					$0.15f_{ctd}/f_{ywd}$	$0.3f_{ctd}/f_{ywd}$
$V_{d,\,max}$		$0.22\times f_{cd}\times b_w\times d$	$0.85\times b_w\times d\times f_{ck}^{0.5}$		$0.25\times f_{cd}\times b_w\times d$	$0.22\times f_{cd}\times b_w\times d$
$c_{c,\,min}$				20 mm	20 mm	25 mm
χ	1	1	0.35			

b_h: beam section height, $b_{h,\,min}$: minimum beam section height, $b_{h,\,max}$: maximum beam section height, b_w: beam section width, $b_{w,\,min}$: minimum beam section width, $b_{w,\,max}$: maximum beam section width, $c_{c,\,min}$: minimum concrete cover, c_{wp}: column section width perpendicular to beam direction, d: effective beam section height, f_{ctd}: design tensile strength of concrete, f_{yd}: design yield strength of reinforcing steel, f_{ywd}: design yield strength of transverse reinforcement, $l_{c,\,min}$: minimum confinement zone length, l_n: net beam length, s_{max}: maximum transverse bar spacing at confinement zone, t_{slab}: slab thickness, $V_{d,\,max}$: maximum design shear force, ρ_{min}: minimum tensile reinforcement ratio, ρ_{max}: maximum tensile reinforcement ratio, $\rho_{t,\,min}$: minimum transverse reinforcement ratio, Φ_l: longitudinal reinforcing bar diameter, $\Phi_{l,\,min}$: minimum longitudinal reinforcing bar diameter, $\Phi_{t,\,min}$: minimum transverse reinforcing bar diameter, Θ_{max}: maximum tension to compression reinforcement ratio at beam support, χ: cracked section rigidity coefficient

ing capacity design principles (e.g., "tr_0018_dch" and "tr_post18_dch"), capacity design bending moments in columns, in which the strong column - weak beam principle is satisfied, and capacity design shear forces in beams and columns are included into the design forces before calculating the reinforcements. For longitudinal reinforcement design of beams, an empirical formula[2] providing not to check beam deflection is used to calculate the required reinforcement area on the top and bottom sides of the section under uniaxial bending moments while also considering the maximum tension-to-compression reinforcement ratio at beam supports, as enforced by seismic design codes (see Θ_{max} in Table 4).

In the case of columns, several design tables were generated for various reinforcing steel grades and axial load ratios using a custom reinforcement area calculator developed for this study based on the theoretical formulations presented in Topçu (2014). This calculator employs an iterative Newton-Raphson method to solve the equilibrium and compat-

[2] The transition limit from a single to a doubly reinforced beam section is defined by a reinforcement ratio (ρ) value of $0.235\times0.235\times\frac{f_{cd}}{f_{yd}}$ (see TS500-1984 and Ersoy et al. 2010), where f_{cd} and f_{yd} denote the design compressive strength of concrete and the design yield strength of reinforcement, respectively.

ibility equations and determines the required longitudinal reinforcement area by assuming an equivalent rectangular concrete stress block and uniformly distributed reinforcing bars throughout the section. For the transverse reinforcement design, the provisions of TS500-1984 and TS500-2000 are applied using the calculated design shear forces. In the "tr_post18_dch" and "tr_post18_dcm" design classes, these shear forces are further evaluated by considering overstrength factors, as mandated in TBEC-2018. Once the required longitudinal and transverse reinforcements are determined, they are configured according to available steel diameters and reinforcement detailing practices, ensuring that all design criteria are satisfied. These reinforcements are then uniformised and adjusted to align with construction practices. For instance, the same reinforcement configuration is used at adjacent beam span ends to ensure practical constructability.

After determining reinforcements, local ductility checks (e.g., verification of maximum longitudinal reinforcement ratios) are performed to ensure compliance with seismic design requirements. If a section fails to meet verification checks or lacks a feasible reinforcement configuration, its dimensions are increased, and the design process following preliminary sizing is repeated. This iterative process continues until a valid design solution is achieved. However, if the section reaches its maximum allowable dimensions without satisfying the design criteria, the originally assigned material properties or structural element types are revised. Any such modification requires repeating the entire design process, including preliminary sizing, until a feasible solution is attained.

Finally, quality-based modifications are applied to the design properties of beams and columns by multiplying with quality factors, which are defined based on the prescribed construction quality level. These quality factors are randomly sampled for each structural component using predefined probability distributions (e.g. quality.json[3]). Specifically, the design values for stirrup spacing, concrete cover, material strengths, and reinforcement ratios are adjusted to reflect expected in-situ values. These adjusted values are then used in the numerical models. Furthermore, construction quality in the framework affects bond-slip factors that are used to characterise plastic hinge properties in beams and columns, as well as the type of beam-column joint model (e.g., rigid, elastic, or inelastic), which are critical in the general structural response.

The quality-based modification process is particularly important for the "tr_7599" design class, due to widespread low quality and illegal constructions of the time. For this design class, it has been assumed that buildings undergone through engineering design process (based on a seismic design regulations), but the designs were not respected during the construction. In particular, we consider that the buildings simulated under the "low" and "moderate" construction quality levels collectively provide a reasonable representation of non-code compliant construction practices. Based on this assumption, the quality-based design modification step was calibrated to better align with the sampling outputs with the observed in-site properties. In this regard, the expected (mean) material strengths, stirrup spacings, and longitudinal reinforcement ratios of elements were calibrated according to the statistical data reported by Bal et al. (2008) and Ozmen et al. (2015).

[3] Available on the following GitHub repository:
https://github.com/builtenvdata/simulateddesign/blob/main/simdesign/rcmrf/bdim/tr_post18_dch/data/quality.json.

3.4 Numerical modelling development

Once the iterative design procedure is completed and quality adjustments are applied, the framework converts the building design data stored in BDIM into 3D non-linear structural models in OpenSees. For the sake of brevity, the numerical modelling procedure adopted in the framework is summarised below; a more comprehensive explanation can be found in Ozsarac et al. (2025).

The current version of the framework employs lumped plasticity approach to simulate non-linear behaviour in frame elements. At the element ends, *zeroLength* elements are introduced to model plastic hinge formation, considering rigid joint offsets. Flexural behaviour in beams is represented with a single rotational spring, while columns feature two rotational springs for each orthogonal direction. More specifically, the *Hysteretic* uniaxial material model in OpenSees is used to define moment-rotation relationships, with yielding moment and yielding rotation capacities are calculated following Panagiotakos and Fardis (2001) and Eurocode 8 – Part 3 (CEN 2005). Additional backbone parameters are derived from Haselton et al. (2016) and ASCE/SEI – 2017 (ASCE, 2017). The bond-slip factor set by the quality model is integrated into plastic rotation capacity, thus ensuring that construction quality effects are accounted for in the hinge properties. While axial-flexural interaction in columns is not explicitly considered in this modelling approach, the backbone curve parameters are determined considering the axial force corresponding to the specified seismic load combination. Additionally, although alternative modelling approaches describing the moment–rotation behaviour of frame elements specific to Turkish RC construction are available in the literature (e.g., Inel and Ozmen 2006; Kian et al. 2025) the current numerical modelling module is designed to be general. It encompasses all implemented design classes to ensure consistency and broad applicability across different regions. Analysts looking to implement more specific numerical modelling strategies can do so by adding these methods to the BNSM module through the collaborative framework available via GitHub.

In cases where capacity design principles are not enforced (e.g., "tr_7599"), shear failure in columns is explicitly modelled using shear springs with zero-length elements. The framework adopts the *LimitState* model with the *ThreePoint* limit curve Elwood (2004) to simulate shear degradation, with displacement ductility-based degradation curves following Sezen and Moehle (2004). Shear strength is computed using the ASCE/SEI – 2017 (ASCE, 2017) model, an extension of Sezen and Moehle (2004). The initial and post-peak stiffness of the shear response is determined using formulations from LeBorgne and Ghannoum (2014) and Shoraka and Elwood (2013), respectively.

Beam-column joints are represented using the *zeroLength* elements positioned between a central joint node and corresponding floor nodes. The central joint nodes establish connectivity between beams and columns and carry structural mass, whereas the floor nodes are constrained by a rigid diaphragm to account for slab behaviour. Rotational flexibility is incorporated for the two horizontal axes, with joints categorised as inelastic, elastic, or rigid, depending on the quality model. The moment-rotation behaviour of inelastic joints is defined using *Hysteretic* uniaxial material, with material parameters obtained from O'Reilly and Sullivan (2019) for different joint locations, including roof, interior, and exterior joints. Elastic joint stiffness is obtained from the initial branches of backbone curves.

4 Example applications

Two example applications were carried out to examine the Turkish RC frame design classes that have been integrated into the framework. The first application involves generating building portfolios for each design class at a specific location in Istanbul and comparing their structural performance based on the results of non-linear pushover analyses. This example also demonstrates the framework's capability to capture the building-to-building variability introduced by uncertainties in the aforementioned secondary attributes and geometry variables, thereby providing insight into the realistic performance of representative buildings from different construction periods. In the second application, fragility curves and loss-related outcomes of the design classes are investigated.

4.1 Portfolio comparison evaluation of design classes for a specific location in Istanbul

In the first example application, 100 different 4-storey RC frame buildings were simulated and subjected to non-linear pushover analyses for each design class listed in Table 5. The design lateral force coefficients, β, were determined assuming that buildings are located on a stiff sandy soil site in the Zeytinburnu district of Istanbul. The fundamental period of buildings was assumed to be approximately 0.64 s, which was estimated using Eq. 4.27 in TBEC-2018 with the assumed building height of 12 m. The probabilities of material grades and construction quality levels (categorised as 1: high, 2: moderate, 3: low) were assigned based on engineering judgment, according to the construction practices of the time period defining each design class. All other input parameters were taken as the default values[4] in each design class. Although the use of moderate ductility classes ("tr_0018_dcm" and "tr_post18_dcm") is not permitted for the buildings in this region, they were included in the analyses to make a comparison. Additionally, "eu_cdl" and "eu_cdh" design classes were incorporated into the comparison by using the same β values of "tr_7599" and "tr_0018_dch" classes, along with their respective default input parameters.

Based on the building portfolio simulations, Fig. 5 illustrates example outputs from the BCIM database for the design class of "tr_7599". The histograms illustrate the variability introduced by the sampling of both secondary design attributes and geometry variables. A diverse range of slab, beam, and column types were generated, reflecting the inherent variability in construction typologies. Similarly, the variation in material grade and construction quality level reflects the differing characteristics across the simulated portfolio. The geometry variables also exhibit notable variability, as seen in the distributions of layout ID, storey heights, and bay widths in both the X and Y directions. In addition, derived properties such as floor area, floor aspect ratio, and total storey height, computed based on the sampled geometry variables, showcase the diversity within the portfolio. These sampling outputs highlight the framework's capability to generate a wide range of realistic configurations consistent with observations from actual construction data reported in previous studies (Azak et al. 2014; Bal et al. 2008; Meral 2019; Ozmen et al. 2015).

Following the generation of the building portfolios, non-linear pushover analyses were performed in both the X and Y directions for all buildings. Figure 6 represents a compari-

[4] Available on the following GitHub repository:https://github.com/builtenvdata/simulated-design/blob/main/simdesign/rcmrf/bcim/data/tr_post18_dch.json.

Table 5 Input parameters for the example application

Design Class	β	Concrete Grade (Probability)	Steel Grade (Probability)	Quality [1, 2, 3]
eu_cdl	0.064	["C14", "C19", "C25"]	["S240", "S400", "S500"]	[0.60, 0.30, 0.10]
		[0.40, 0.40, 0.20]	[0.20, 0.70, 0.10]	
eu_cdh	0.086	["C20", "C25", "C30", "C35"]	["S400", "S500"]	[0.60, 0.30, 0.10]
		[0.30, 0.45, 0.20, 0.05]	[0.10, 0.90]	
tr_7599	0.064	["C14", "C16", "C18", "C20", "C25"]	["S220", "S420"]	[0.10, 0.30, 0.60]
		[0.40, 0.25, 0.20, 0.10, 0.05]	[0.90, 0.10]	
tr_0018_dch	0.086	["C20", "C25", "C30", "C35"]	["S420"]	[0.60, 0.30, 0.10]
		[0.40, 0.40, 0.15, 0.05]	[1.0]	
tr_post18_dch	0.09	["C25", "C30", "C35"]	["B420C", "B500C"]	[0.80, 0.10, 0.10]
		[0.45, 0.45, 0.10]	[0.90, 0.10]	
tr_0018_dcm	0.086	["C20", "C25", "C30", "C35"]	["S420"]	[0.60, 0.30, 0.10]
		[0.40, 0.40, 0.15, 0.05]	[1.0]	
tr_post18_dcm	0.09	["C25", "C30", "C35"]	["B420C", "B500C"]	[0.80, 0.10, 0.10]
		[0.45, 0.45, 0.10]	[0.90, 0.10]	

son of the median pushover curves across the seven evaluated design classes. To ensure a meaningful comparison, base shear and roof displacement values were normalised by the corresponding structural weight and building height, respectively. The results demonstrate a clear trend of increasing lateral strength and deformation capacity in line with the evolution of seismic design codes and construction practices. The buildings constructed in the post-2000 period exhibit substantially higher strength and deformation capacity than those built prior to 2000. This improvement is attributed not only to better construction quality but also to fundamental shifts in seismic design philosophy. Notably, the adoption of capacity design principles, stricter design provisions and the consideration of higher seismic load levels are critical factors here in improving both the strength and deformation capacities of the buildings. A considerable difference in ductility level was observed between buildings designed for high ductility and those with moderate ductility levels, as expected. Importantly, the median pushover curve of the buildings designed according to the "eu_cdl" class exhibits more strength compared to those designed under the "tr_7599" class, however, may exhibit lower displacement capacity, as observed on the pushover curves for y-direction.

4.2 Fragility and loss-based comparison of the "tr_7599" and "tr_0018_dch" design classes

Having generated building models and attaining their pushover curves in the previous example, collapse fragility curves of the "tr_7599" and "tr_0018_dch" design classes were investigated. To this end, equivalent single-degree-of-freedom (SDOF) models were derived using the median capacity curves and were then subjected to non-linear time history analyses using the ground motion records employed in the ESRM20 study. From these results, fragility curves were developed with the cloud analysis approach (Jalayer et al. 2017), and the results are shown in Fig. 7 (for PGV on the left, and for SA on the right). As expected, significant differences in damage probabilities were observed between the "tr_7599" and "tr_0018_dch" design classes.

For comparison, reference fragility curves available from the literature via Kircil and Polat (2006) for SA, and Akkar et al. (2005) and Erberik (2008) for PGV were also included. The building models in Akkar et al. (2005) and Erberik (2008) were developed based on the characteristics of buildings affected by the 1999 Düzce earthquake, whereas the models in the study by Kircil and Polat (2006) were developed in accordance with the 1975 seismic code, taking into account the low in-situ material strength and neglecting the confinement effect of transverse reinforcements due to the poor quality of the building stock. In Akkar et al. (2005), equivalent strut elements were included to represent the effect of infill walls. Erberik (2008) examined both modelling cases (with and without infill walls), however, we used the collapse fragility curve for the models without infill wall since it is also the case for our models. Similarly, Kircil and Polat (2006) did not include infill walls into their models. Additionally, since Erberik (2008) proposed fragility curves for 3 and 5 storey buildings seperately, average of the fragility curve parameters have been used. The fragility curve comparisons indicate that median intensity values are relatively close to each other whereas the dispersions are higher in the case of this study. This is not only due to employing higher amount of models but also due to the considerations of broader range of variabilities in material and geometrical properties, as explained in the previous sections.

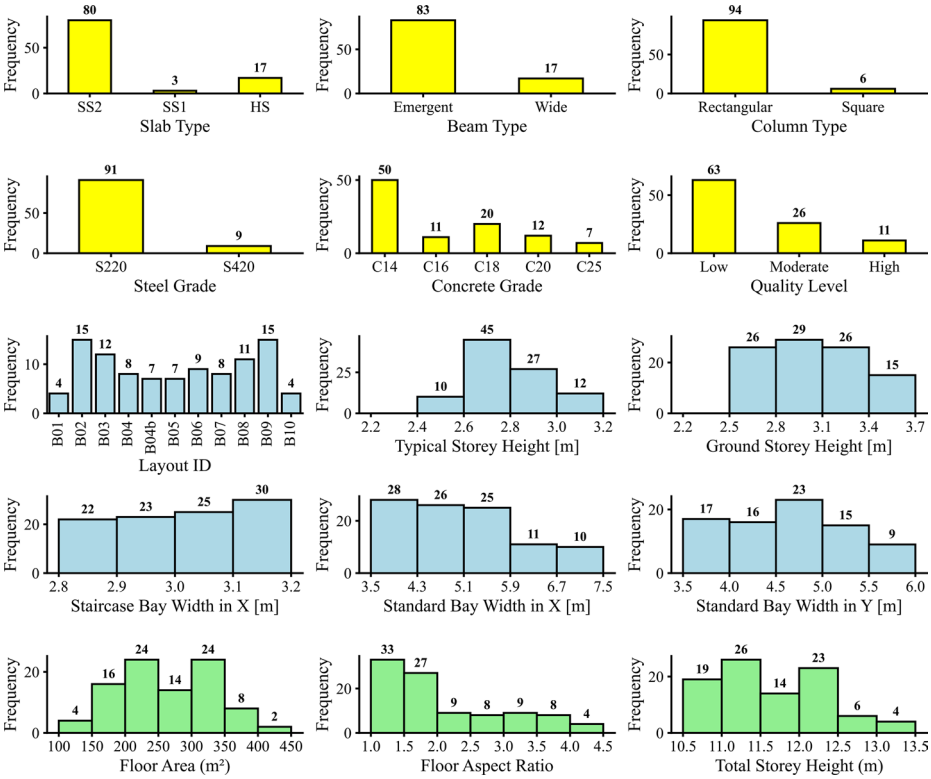

Fig. 5 Example BCIM data histograms for the "tr_7599" design class. (Yellow bars: sampled design attributes; light-blue bars: primary geometrical variables; and light-green bars: derived geometrical properties)

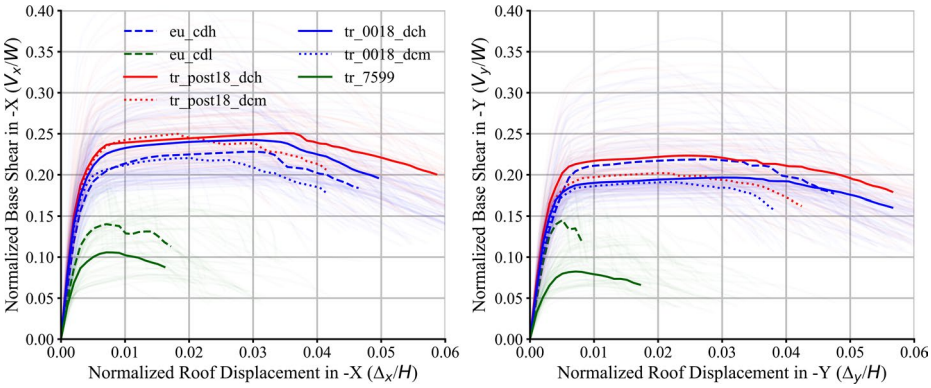

Fig. 6 Normalised pushover curves for the simulated buildings in each design class, shown for both in X and Y directions

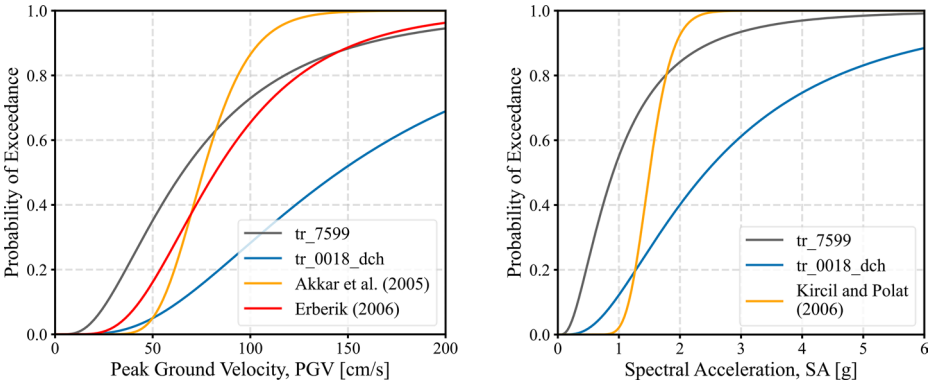

Fig. 7 Comparison of the collapse fragility curves of the "tr_7599" design class with those of the "tr_0018_dch" design class and a reference fragility curves from the literature for SA on the left and PGV on the right

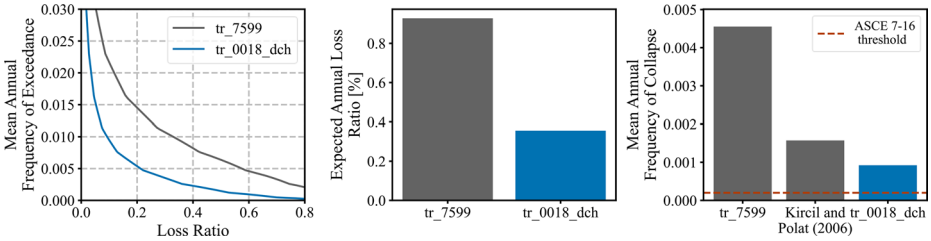

Fig. 8 Mean annual frequency of exceedance (MAFE) vs. loss ratio distribution (on the left), expected annual loss ratios in percent (in the middle), and mean annual frequency of collapse (on the right) values for the considered design classes

Subsequently, vulnerability curves of the design classes were derived using the damage model proposed by Martins and Silva (2021). These curves were then integrated with seismic hazard curve of the region, calculated for the SA(0.70s) intensity measure using the OpenQuake engine (Silva et al. 2014) to produce loss hazard curves and compute the expected annual loss ratios and mean annual frequency of collapse (MAFC) values as illustrated in Fig. 8. The results show that the RC frame buildings constructed before 2000 in Türkiye has significantly high annual loss ratio and annual frequency of collapse values, which indicates the significantly high seismic risk of the investigated building typology in the region.

Additionally, the MAFC threshold (0.0002, corresponding to 1% probability of collapse in 50 years) recommended by ASCE/SEI 7–16 (ASCE, 2016) for the design of new buildings was also included to the figure to make a comparison. The comparison revealed that the threshold value suggested by ASCE is considerably lower than the value calculated for the "tr_0018_dch" design class. Although infill walls were not included in the numerical models, and their possible beneficial contribution to structural performance is therefore not captured in the results, it is highly likely that the ASCE threshold would still remain lower even if infill were considered. Furthermore, this exercise to compute fragility curves and estimate annualised losses could also be extended to entire cities or regions with sufficiently

detailed hazard and exposure information, allowing for comparison with past studies such as (Ansal et al. 2009; Hancilar et al. 2020) or a more regional view of seismic risk, and how this SimDesign's approach to vulnerability modelling can be utilised.

5 Summary and conclusions

This study introduced a country-specific extension of the Built Environment Data's (BED) SimDesign framework, specifically for RC frame buildings in Türkiye. By incorporating both historical and modern Turkish seismic design codes, relevant RC design provisions from the TS500 series, and available statistical data on construction practices, the framework establishes a robust methodology for generating realistic building portfolios. These portfolios effectively capture the evolution of seismic design philosophy and reflect the inherent variability in the Turkish building stock.

In this regard, five design classes were defined in the framework based on construction period and ductility level, with detailed code-based rules integrated accordingly. Additionally, mean material strength values, longitudinal and translational reinforcements were calibrated using available literature data to account for the effects of poor construction quality, which is common in buildings constructed prior to 2000. To evaluate the performance of Turkish RC frame classes, example applications were performed through non-linear pushover and dynamic analyses on the simulated buildings. The results confirmed that the generated portfolios successfully capture the variability in structural attributes such as geometry, material grade and construction quality level. Moreover, a clear trend of increasing structural capacity and ductility was observed across design classes, which is in line with the progressive evolution of seismic code requirements and construction practices over time. Furthermore, the agreement between the fragility curves derived from the example application and the literature further supports the proposed method.

While the statistical data used in Turkish design classes provided a strong foundation, further refinement is needed to enhance model accuracy. The availability of comprehensive and up-to-date statistical data on material properties and geometrical characteristics of Turkish RC buildings would significantly improve to achieve more representative models. In particular, material strength data that include both the one used in the design phase and in-situ strength values (may be obtained through lab tests or rapid field assessment methods) would allow for a more accurate representation of construction quality at the material level. Another significant issue in the pre-2000 RC building stock is the addition of unauthorised storeys. However, due to the lack of data quantifying the extent of this problem such as how many unauthorised storeys are typically added, what percentage of buildings are affected, or what type of approach should be followed to model these additions, this problem was not explicitly addressed within the current framework. Advancing these aspects requires collaboration and support from the academic and professional community.

In conclusion, the developed framework offers a practical and adaptable tool for generating time- and region-specific RC building portfolios in Türkiye, thereby providing the base for enhanced future vulnerability models. In the long term, the framework holds significant potential to inform large-scale seismic risk assessments, guide risk reduction strategies, and even contribute to the development of future seismic codes in the country.

Supplementary Information The online version contains supplementary material available at https://doi.org/10.1007/s10518-025-02301-y.

Author contributions All authors contributed to the study conception and design. Material preparation, data collection and analysis were performed by Serkan Hasanoğlu. The first draft of the manuscript was written by Serkan Hasanoğlu, and Volkan Ozsarac and Gerard J. O'Reilly commented and edited on subsequent versions of the manuscript. All authors read and approved the final manuscript.

Funding The work presented herein was carried out with financial support from the European Union through the Geo-INQUIRE (Grant Agreement No. 101058518) and EPOS-ON (Grant Agreement No.101131592) projects.

Data availability The data and material developed as part of this study are freely available on Github at: https://github.com/builtenvdata/simulated-design/.

Code availability The code developed as part of this study is freely available on Github at: https://github.com/builtenvdata/simulated-design/.

Declarations

Competing interests The authors have no conflicts of interest to declare that are relevant to the content of this article.

References

Akkar S, Sucuoglu H, Yakut A (2005) Displacement-Based fragility functions for Low- and Mid-rise ordinary concrete buildings. Earthq Spectra. https://doi.org/10.1193/1.2084232

Ansal A, Akinci A, Cultrera G, Erdik M, Pessina V, Tönük G, Ameri G (2009) Loss Estimation in Istanbul based on deterministic earthquake scenarios of the Marmara sea region (Turkey). Soil Dyn Earthq Eng 29(4):699–709. https://doi.org/10.1016/j.soildyn.2008.07.006

ASCE/SEI 41 – 17 (2017) Seismic evaluation and retrofit of existing buildings (ASCE/SEI 41 – 17). Seismic rehabilitation of existing buildings (Asce/Sei 41 – 17), vol 41. Issue 17). American Society of Civil Engineers

ASCE/SEI 7–16 (2016) Minimum design loads and associated criteria for buildings and other structures, 7th edn. American Society of Civil Engineers. https://doi.org/10.1061/9780784414248

Azak TE, Ay BÖ, Akkar S (2014) A statistical study on geometrical properties of Turkish reinforced concrete building stock. 2nd European Conference on Earthquake Engineering.

Bal IE, Crowley H, Pinho R, Gülay FG (2008) Detailed assessment of structural characteristics of Turkish RC Building stock for loss assessment models. Soil Dyn Earthq Eng 28(10–11):914–932. https://doi.org/10.1016/j.soildyn.2007.10.005

Bayraktar A, Altunişik AC, Pehlivan M (2013) Performance and damages of reinforced concrete buildings during the October 23 and November 9, 2011 Van, Turkey, earthquakes. Soil Dyn Earthq Eng 53:49–72. https://doi.org/10.1016/j.soildyn.2013.06.004

Binici B, Yakut A, Kadas K, Demirel O, Akpinar U, Canbolat A, Yurtseven F, Oztaskin O, Aktas S, Canbay E (2023) Performance of RC buildings after Kahramanmaraş earthquakes: lessons toward performance-based design. Earthq Eng Eng Vib 22(4):883–894. https://doi.org/10.1007/s11803-023-2206-8

Borzi B, Pinho R, Crowley H (2008) Simplified pushover-based vulnerability analysis for large-scale assessment of RC buildings. Eng Struct 30(3):804–820. https://doi.org/10.1016/j.engstruct.2007.05.021

Cansiz S (2022) Türkiye'de Kullanılan deprem Yönetmeliklerinin Özellikleri ve deprem Hesabının Değişimi. Uluslararası Muhendislik Arastirma Ve Gelistirme Dergisi 14(1):58–71. https://doi.org/10.29137/umagd.948025

CEN (2005) Eurocode 8: Design of structures for earthquake resistance—Part 3: Assessment and retrofitting of buildings. In EN 1998-3:2005.

Crowley H, Despotaki V, Rodrigues D, Silva V, Toma-Danila D, Riga E, Karatzetzou A, Fotopoulou S, Zugic Z, Sousa L, Ozcebe S, Gamba P (2020) Exposure model for European seismic risk assessment. Earthq Spectra 36(1suppl):252–273. https://doi.org/10.1177/8755293020919429

Crowley D, Despotaki, Rodrigues, Martins, Silva, Romão, Pereira W, Danciu (2021a). European Seismic Risk Model (ESRM20). Eucentre. https://doi.org/10.7414/EUC-EFEHR-TR002-ESRM20

Crowley H, Despotaki V, Silva V, Dabbeek J, Romão X, Pereira N, Castro JM, Daniell J, Veliu E, Bilgin H, Adam C, Deyanova M, Ademović N, Atalic J, Riga E, Karatzetzou A, Bessason B, Shendova V, Tiganescu A, Hancilar U (2021b) Model of seismic design lateral force levels for the existing reinforced concrete European Building stock. Bull Earthq Eng 19(7):2839–2865. https://doi.org/10.1007/s10518-021-01083-3

D'Ayala D, Meslem A, Vamvatsikos D, Porter K, Rossetto T, Silva V (2015) GEM Global earthquake model vulnerability and loss modelling GEM Technical report 2014-12 V1.0.0 Guidelines for Analytical Vulnerability Assessment-Low/Mid-Rise. https://doi.org/10.13117/GEM.VULN-MOD.TR2014.12

Del Gaudio C, Ricci P, Verderame GM, Manfredi G (2015) Development and urban-scale application of a simplified method for seismic fragility assessment of RC buildings. Eng Struct 91:40–57. https://doi.org/10.1016/j.engstruct.2015.01.031

Elwood KJ (2004) Modelling failures in existing reinforced concrete columns. Can J Civ Eng 31(5):846–859. https://doi.org/10.1139/L04-040

Erberik MA (2008) Fragility-based assessment of typical mid-rise and low-rise RC buildings in Turkey. Eng Struct 30(5):1360–1374. https://doi.org/10.1016/j.engstruct.2007.07.016

Erdik M (2001) Report on 1999 Kocaeli and Duzce (Turkey) earthquakes. Struct Control Civil Infrastructure Eng 149–186. https://doi.org/10.1142/9789812811707_0018

Ersoy U, Ozcebe G, Tankut T (2010) Reinforced Concrete.

Hancilar U, Taucer F, Corbane C (2013) Empirical fragility functions based on remote sensing and field data after the 12 January 2010 Haiti earthquake. Earthq Spectra 29(4):1275–1310. https://doi.org/10.1193/121711EQS308M

Hancilar U, Sesetyan K, Cakti E (2020) Comparative earthquake loss estimations for high-code buildings in Istanbul. Soil Dyn Earthq Eng 129. https://doi.org/10.1016/j.soildyn.2019.105956

Haselton CB, Liel AB, Taylor-Lange SC, Deierlein GG (2016) Calibration of model to simulate response of reinforced concrete beam-columns to collapse. ACI Struct J 113(6):1141–1152. https://doi.org/10.14359/51689245

Ilki A, Celep Z (2012) Earthquakes, existing buildings and seismic design codes in Turkey. Arab J Sci Eng 37(2):365–380. https://doi.org/10.1007/s13369-012-0183-8

Inel M, Ozmen HB (2006) Effects of plastic hinge properties in nonlinear analysis of reinforced concrete buildings. Eng Struct 28(11):1494–1502. https://doi.org/10.1016/j.engstruct.2006.01.017

Jalayer F, Ebrahimian H, Miano A, Manfredi G, Sezen H (2017) Analytical fragility assessment using unscaled ground motion records. Earthq Eng Struct Dynamics 46(15):2639–2663. https://doi.org/10.1002/eqe.2922

Kappos AJ, Stylianidis KC, Pitilakis K (1998) Development of seismic risk scenarios based on a hybrid method of vulnerability assessment. Nat Hazards. https://doi.org/10.1023/A:1008083021022

Kian N, Demir U, Ates AO, Celik OC, Ilki A (2025) Seismic testing and modeling of Full-Scale substandard RC columns retrofitted with sprayed GFRM with and without basalt mesh under high axial compression and shear demand. J Compos Constr. https://doi.org/10.1061/JCCOF2.CCENG-5227

Kircher CA, Reitherman RK, Whitman RV, Arnold C (1997) Estimation of earthquake losses to buildings. Earthq Spectra 13(4):703–720. https://doi.org/10.1193/1.1585976

Kirçil MS, Polat Z (2006) Fragility analysis of mid-rise R/C frame buildings. Eng Struct 28(9):1335–1345. https://doi.org/10.1016/j.engstruct.2006.01.004

LeBorgne MR, Ghannoum WM (2014) Calibrated analytical element for lateral-strength degradation of reinforced concrete columns. Eng Struct 81:35–48. https://doi.org/10.1016/j.engstruct.2014.09.030

Martins L, Silva V (2021) Development of a fragility and vulnerability model for global seismic risk analyses. Bull Earthq Eng 19(15):6719–6745. https://doi.org/10.1007/s10518-020-00885-1

McKenna F, Scott MH, Fenves GL (2010) Nonlinear Finite-Element analysis software architecture using object composition. J Comput Civil Eng 24(1):95–107. https://doi.org/10.1061/(ASCE)CP.1943-5487.0000002

Meral E (2019) Evaluation of structural properties of existing Turkish RC Building stock. Iran J Sci Technol Trans Civil Eng 43(3):445–462. https://doi.org/10.1007/s40996-018-0207-z

Nafeh AMB, O'Reilly GJ (2023) Simplified pushover-based seismic risk assessment methodology for existing infilled frame structures. Bull Earthq Eng 21(4):2337–2368. https://doi.org/10.1007/s10518-022-01600-y

Nafeh AMB, O'Reilly GJ (2024) Fragility functions for non-ductile infilled reinforced concrete buildings using next-generation intensity measures based on analytical models and empirical data from past earthquakes. Bull Earthq Eng. https://doi.org/10.1007/s10518-024-01955-4
O'Reilly GJ, Sullivan TJ (2018) Quantification of modelling uncertainty in existing Italian RC frames. Earthq Eng Struct Dynamics 47(4):1054–1074. https://doi.org/10.1002/eqe.3005
O'Reilly GJ, Sullivan TJ (2019) Modeling techniques for the seismic assessment of the existing Italian RC frame structures. J Earthquake Eng 23(8):1262–1296. https://doi.org/10.1080/13632469.2017.1360224
Ozcebe G, Yucemen MS, Yakut A (2003) Seismic vulnerability assessment procedure for low- to medium-rise reinforced concrete buildings.
Ozmen HB, Inel M, Senel SM, Kayhan AH (2015) Load carrying system characteristics of existing Turkish RC Building stock. Int J Civil Eng
Ozsarac V, Pereira N, Mohamed H, Romão X, O'Reilly GJ (2025) The built environment data framework for simulated design and vulnerability modelling in earthquake engineering.
Panagiotakos TB, Fardis MN (2001) A displacement-based seismic design procedure for RC buildings and comparison with EC8. Earthq Eng Struct Dynamics 30(10):1439–1462. https://doi.org/10.1002/eqe.71
Reilinger R, McClusky S, Vernant P, Lawrence S, Ergintav S, Cakmak R, Ozener H, Kadirov F, Guliev I, Stepanyan R, Nadariya M, Hahubia G, Mahmoud S, Sakr K, ArRajehi A, Paradissis D, Al-Aydrus A, Prilepin M, Guseva T, Karam G (2006) GPS constraints on continental deformation in the Africa-Arabia-Eurasia continental collision zone and implications for the dynamics of plate interactions. J Geophys Res Solid Earth, 111(B5), 2005JB004051. https://doi.org/10.1029/2005JB004051
Rossetto T, Elnashai A (2003) Derivation of vulnerability functions for European-type RC structures based on observational data. Eng Struct 25(10):1241–1263. https://doi.org/10.1016/S0141-0296(03)00060-9
Ruggieri S, Calò M, Cardellicchio A, Uva G (2022a) Analytical-mechanical based framework for seismic overall fragility analysis of existing RC buildings in town compartments. Bull Earthq Eng 20(15):8179–8216. https://doi.org/10.1007/s10518-022-01516-7
Ruggieri S, Chatzidaki A, Vamvatsikos D, Uva G (2022b) Reduced-order models for the seismic assessment of plan-irregular low-rise frame buildings. Earthq Eng Struct Dynamics 51(14):3327–3346. https://doi.org/10.1002/eqe.3725
Sezen H, Moehle J (2004) Shear strength model for lightly reinforced concrete columns. J Struct Eng 130(11):1692–1703. https://doi.org/10.1061/(asce)0733-9445(2004)130:11(1692)
Shoraka MB, Elwood KJ (2013) Mechanical model for non-ductile reinforced concrete columns. J Earthquake Eng 17(7):937–957. https://doi.org/10.1080/13632469.2013.794718
Silva V, Crowley H, Pagani M, Monelli D, Pinho R (2014) Development of the openquake engine, the global earthquake model's open-source software for seismic risk assessment. Nat Hazards 72(3):1409–1427. https://doi.org/10.1007/s11069-013-0618-x
TBEC (1975) Afet Bölgelerinde Yapılacak Yapılar Hakkında Yönetmelik. Resmi Gazete
TBEC (1998) Afet Bölgelerinde Yapılacak Yapılar Hakkında Yönetmelik. Resmi Gazete
TBEC (2007) Deprem Bolgelerinde Yapilacak Binalar Hakkinda Esaslar. Resmi Gazete
TBEC (2018) Deprem Etkisi altında binaların tasarımı için Esaslar. Resmi Gazete
Topçu A (2014) Betonarme2000: Çokgen Kesitli Kolon Boyuna Donatısının Hesabı Teori ve Örnekler.
TS500 (1984) Requirements for design and construction of reinforced concrete structures. Turkish Standards Institution, Ankara
TS500 (2000) Requirements for design and construction of reinforced concrete structures. Turkish Standards Institution, Ankara
Ucar T, Merter O, Duzgun M (2015) Determination of lateral strength and ductility characteristics of existing mid-rise RC buildings in Turkey. Computers Concrete 16(3):467–485. https://doi.org/10.12989/cac.2015.16.3.467
United State Geological Survey (USGS). (2024) [Online post]. https://earthquake.usgs.gov/storymap/index-turkey2023.html
Verderame GM, Polese M, Mariniello C, Manfredi G (2010) A simulated design procedure for the assessment of seismic capacity of existing reinforced concrete buildings. Adv Eng Softw 41(2):323–335. https://doi.org/10.1016/j.advengsoft.2009.06.011
Yakut A, Sucuoğlu H, Binici B, Canbay E, Donmez C, İlki A, Caner A, Celik OC, Ay BÖ (2022) Performance of structures in İzmir after the Samos Island earthquake. Bull Earthq Eng 20(14):7793–7818. https://doi.org/10.1007/s10518-021-01226-6
Yilmaz Z, Altunişik AC, Taciroglu E, Günaydin M, Okur FY, Sunca F, Şişman R, Aslan B, Sezdirmez T (2024) Regional Building damage survey data on the 2023 Kahramanmaraş, Türkiye, earthquakes. ASCE OPEN: Multidisciplinary J Civil Eng 2(1). https://doi.org/10.1061/AOMJAH.AOENG-0041
Yuzbasi J (2024) Post-Earthquake damage assessment: field observations and recent developments with recommendations from the Kahramanmaraş earthquakes in Türkiye on February 6th, 2023 (Pazarcık M7.8 and Elbistan M7.6). J Earthquake Eng 1–26. https://doi.org/10.1080/13632469.2024.2353864

Zhu M, McKenna F, Scott MH (2018) OpenSeesPy: python library for the opensees finite element framework. SoftwareX 7:6–11. https://doi.org/10.1016/j.softx.2017.10.009

Authors and Affiliations

Serkan Hasanoğlu[1,2] · Volkan Ozsarac[1,2] · Gerard J. O'Reilly[1,2]

✉ Gerard J. O'Reilly
gerard.oreilly@iusspavia.it

[1] Centre for Training and Research on Reduction of Seismic Risk (ROSE Centre), Scuola Universitaria Superiore IUSS di Pavia, Pavia, Italy

[2] European Centre for Training and Research in Earthquake Engineering (EUCENTRE), Pavia, Italy